68th International Astronautical Congress (IAC), Adelaide, Australia, 25-29 September 2017.

IAC-17-A2.6.2

Fluid dynamic in space experiment

Jean Mignot [a]*, Romain Pierre[b], Michael Berhanu[c], Barbara Busset[d], Rémi Roumiguié[e], Henri Bavestrello[f], Stefano Bonfanti[g] , Thomas Miquel[h], Lourdes Oro Marot [i] , Anais Llodra-Perez [j]

[a] *Centre National d'Etudes Spatiales, 18 Avenue Edouard Belin Toulouse France* jean.mignot@cnes.fr
[b] *Airbus Defence and Space Rue des cosmonautes Toulouse France* romain.r.pierre@airbus.com
[c] *Laboratoire MSC UMR7057 CNRS Université Paris Diderot* michael.berhanu@univ-paris-diderot.fr
[d] *Airbus Defence and Space Rue des cosmonautes Toulouse France* barbara.bussetl@airbus.com
[e] *Airbus Defence and Space Rue des cosmonautes Toulouse France* remi.roumiguie@airbus.com
[f] *Airbus Defence and Space Rue des cosmonautes Toulouse France* henri.bavestrello@airbus.com
[g] *Airbus Defence and Space Rue des cosmonautes Toulouse France* stefano.bonfanti@airbus.com
[h] *Airbus Defence and Space Rue des cosmonautes Toulouse France* thomas.miquel@airbus.com
[i] *MEDES, 21 Chemin de la Pelude Toulouse France* Lourdes.OroMarot@cnes.fr
[j] *MEDES, 21 Chemin de la Pelude Toulouse France* Anais.Llodra-Perez@cnes.fr
* Corresponding Author

Abstract

Sloshing phenomena of satellite fuel has become over the last few years a significant disturbance especially for manoeuvring spacecraft with tight performance requirements to ensure. As sloshing can be observed only in 0g domain where capillary forces start dominating the inertial effect, satellite design is mainly based on more or less complex models. Because of the unavailability or inaccessibility of experimental data, these models are often not thoroughly validated.

FLUIDICS (FLUId DynamICs in Space) was a part of the PROXIMA project development during the flight of Thomas Pesquet. The development has been done in close cooperation and funding of Airbus and CNES. The main goal of the experiment is to enable model validation through correlation with measurements. FLUIDICS apparatus is built as a slow rate centrifuge that can establish specific controlled micro-gravity conditions or dedicated excitations on a sample tank. Two cameras offer video recording capability and a dedicated sensor monitors the forces generated by the fluid motion.

For the sloshing part, experimental motion profiles implements several acceleration and speed representative of typical satellite slew manoeuvres and tranquilization phases. Two tanks will be used to study the impact of the filling ratio, representative of the depletion during the satellite lifetime.

Another objective of the FLUIDICS experiment consists in the study of turbulent regimes of surface waves in absence of gravity. Pure capillary waves are excited at the air-water interface in a dedicated tank, by applying sinusoidal or random oscillations. Interface position is locally measured using two incorporated liquid-level probes. Capillary wave turbulence regimes have been observed and analysed through the frequency power spectrum of wave elevation.

Fluidics experiment is still on-board of Columbus ready to be used in the next few months. Innovative perspectives are also foreseen to study new tanks design mitigating the sloshing impact that can be used on the same FLUIDICS setup.

Keywords: fluid dynamics attitude control sloshing wave turbulences

Acronyms/Abbreviations

International Space Station (ISS).
Computational Fluid Dynamic (CFD)
Attitude and Orbit Control System (AOCS)

1. Introduction

The sloshing phenomena impacting the spacecraft dynamic is not a new subject and has triggered a lot of fundamental research in the early 1960 and simplified theoretical model were developed to characterize the fluid motion in spacecraft tank. However for the past twenty years, with the larger amount of fluid that has to be carried aboard spacecraft for an increase lifetime or more recently to deal with new regulations taking care of satellites end of life disposal, sloshing has become an important design driver at satellite level to ensure compliance with the high accuracy pointing performances that satellites may need to deliver. Although the propellant tanks are the main impacted subsystems to limit the sloshing impact, the AOCS is also concerned and it is of great importance to check

that sloshing impact on satellite dynamic does not affect pointing performances. Otherwise the AOCS design would need to be adapted to mitigate the sloshing impact to meet the performance requirements.
Several models and solvers exist to evaluate fluid motion in microgravity. Coupled fluid motion and spacecraft dynamics are simulated using simplified model of the fluid (Abramson theory) tuned for one particular working point. This simplified model is validated for the considered working point by a CFD simulation that is the most accurate method available to simulate fluid motion. Nevertheless experimental data to validate CFD code under 0g domain are missing or are unavailable because of property rights issue [2].

Lastly, two French academic research institutes affiliated with the "Centre National de la Recherche Scientifique" (CNRS), "Matière et Systèmes Complexes" (MSC) at the university Paris Diderot, and the laboratoire de Physique Statistique (LPS) at the "Ecole Normale Supérieure" (ENS) investigate turbulent regimes of capillary waves (French acronym "TOC" for "Turbulence d'Ondes Capillaires") in a microgravity experiment. Wave Turbulence consists in the statistical study of random regimes of dispersive and non-linearly interacting waves. This phenomenon occurs at very different scales in great variety of systems like surface or internal waves in oceanography, Alfven waves in solar-wind plasma, or spin waves in solid state physics. For weak non-linearity, the Weak Turbulence Theory [3] predicts analytically the power spectra of wave elevation, which is not possible at the days for hydrodynamics turbulence. On Earth, random regimes of surface waves at the air water interface can be analysed in the framework of this theory. At large scale the main restoring force is the gravity, whereas at small scale it is the surface tension of the interface (the capillarity). Simultaneous presence of two different restoring mechanisms complicates the analysis of capillary waves regimes (typically for wavelengths smaller than about 17mm) and they are strongly affected by the viscous dissipation. Moreover, the complete validation of Weak Turbulence Theory for capillary waves has been performed using direct numerical simulations only for pure capillary waves [4]. The observation of pure capillary waves becomes possible by operating in microgravity. Parabolic flights were used to investigate this phenomenon with promising results but low frequency could not be resolved accurately because of the short duration of the 0g conditions [5]. Once more ISS appears the only way to get accurate data at low frequency with a long duration in a steady and clean micro gravity environment.

This paper will describe the sloshing phenomena and its impact on pointing performances from real examples and will then present the FLUIDICS experimental setup with a special focus on the capability it offers to study fluid motion in 0g domain. Then the capillary wave turbulence phenomena will be also addressed and discussed.

2. Sloshing phenomena and impact on mission performance

In this section sloshing characteristics that have to be considered for satellite performance synthesis are defined and concrete example of sloshing effects are given to illustrate the interest of this matter.

The dynamic motion of a liquid gas-system can be characterized in three domains, depending on the dominating forces applied to the fluid. Specific dimensionless numbers allow describing the fluid regime and defining the boundary of each fluid motion domain. The Bond number (Bo) usually known as the ratio between inertial forces and capillary forces as defined by (1) is commonly used to determine whether capillary forces are dominating over the inertial force or vice versa.

$$Bo = \frac{gravity\ \ forces}{surface\ tension\ \ forces} = \frac{\rho \gamma h R}{\sigma} \quad (1)$$

Where γ is the acceleration level, ρ the fluid density, σ its surface tension, h and R are respectively the hydrostatic and capillary dimensions.
Fluid motion in satellite tanks is generally characterized by low Bond number values, typically between 0 and 30, that are representative of the rather low acceleration obtained during satellite manoeuvre. Typical satellite angular speeds are considered less than 3 deg/s. Lever arm and tank characteristic dimensions are usually around some tens of centimetres. In this fluid regime, the damping factor is quite low and once excited the slosh amplitude will remain significant for several tens of seconds. During this tranquilization phase, in the case of a high resolution observation mission, images may not be taken to avoid blurriness and sloshing reduces the available mission time.

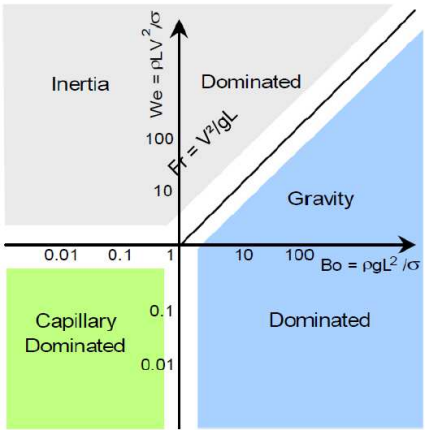

Figure 1: Fluid regime characterization depending on the dominating forces

A flexible spacecraft may have a mode cantilever frequency close to the sloshing and specific analysis may in this case be required to check no resonance could be excited during manoeuvres, which could lead to important mechanical stress on structures.

Validation of tools and models used to design satellites and assess their performances has become a key phase to further improve and reach higher objectives.

3. Sloshing models

Fluid motion is driven by Navier Stokes equations that are a set of non-linear differential equations and requires high computational time to resolve a short sequence. Coupling with complete space craft dynamics to perform closed loop simulation of representative manoeuvres has been explored through a study led by CNES and ESA but is still really challenging and current tools are not fully adapted for such full scale simulation even if current tools are becoming more and more powerful.

Preliminary design and advanced studies for the AOCS are generally based on simplified mass-spring or pendulum model issued from Abramson theory documented in [1] and illustrated on Figure 1:. Several working points are identified to be analysed and model parameters are determined using CFD simulations, an example of which is presented on Figure 2 that simulates the fluid motion by resolving the full Navier Stokes set of equations in 0g domain. Furthermore Abramson model validity domain is limited to the vicinity of the working point so that the fluid behaviour remains linear with small amplitude. However, when the fluid motion becomes non-linear, with for example the apparition of waves in the tank, those models are no more valid. That is why scientists have to tend to a fully close loop simulation to be more representative of those dynamic phases.

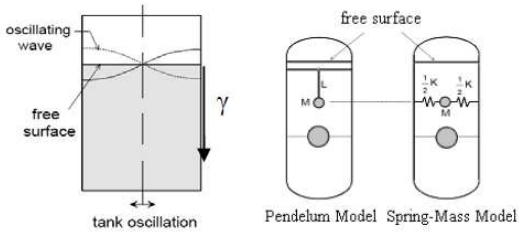

Figure 1: Abramson pendulum and mass-spring models representation

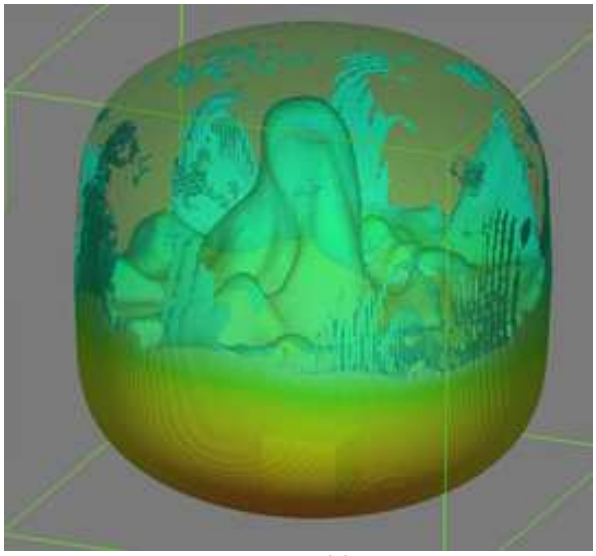

Figure 2: CFD simulation of fluid sloshing inside a spherical tank

Engineers are confident with CFD codes to describe high Bond number maneuvers. In fact, for these regimes of acceleration, the inertial forces are predominant compared to capillary effects. Therefore, it is easier to have access to experimental data on ground and flight data from launchers for validation. On the contrary for the low Bond number, the common weakness of all these more or less complex sloshing models in microgravity is the lack of experimental data to validate their representativeness.

Indeed at lower Bond regimes, capillary forces become as important as inertial forces and sloshing oscillations period increases significantly to reach several tens of seconds as depicted on Figure 3: It is thus impossible to have access to validation data on ground, and some others validation way (0g-flight, drop tower) are discarded due to the need for a long duration test representative of the sloshing characteristic time. The experiment to gather representative test data for sloshing model validation must therefore be done in space and the ISS is the ideal laboratory for it [8].

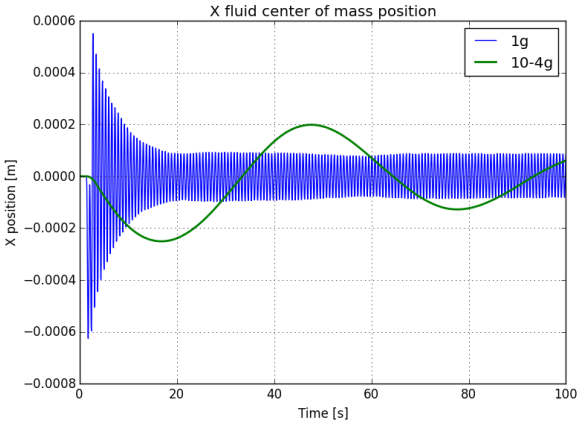

Figure 3: Sloshing period under 1g vs 0g

4. Fluidics setup

4.1 Experimental need definition

A typical slosh speed profile is illustrated on Figure 4 and includes five different phases. The first phase aims at settling the fluid so that the fluid motion starts from a well-known state that can be reproduced in simulation. The second phase is the motion ramp up with a constant acceleration until the nominal rotation speed is reached for the third phase that provides a centrifugal constant (and low) acceleration according to the targeted Bond number. This phase can last a long time so that several slosh periods can be observed, even for long damping durations. Eventually, the fourth phase corresponds to speed reduction down to steady state so that in the fifth phase the fluid tranquilization can be fully investigated.
The fluid slosh is also greatly influenced by the tank filling ratio that has a quite non-linear impact on the fluid behaviour. Therefore this parameter influence needs to be studied and 2 filling ratios were identified of great interest. First the 50% filling ratio representative of the middle of life of the satellite is the most critical in term of sloshing amplitude and secondly the 75% filling ratio representative of the beginning of life is expecting to transmit the most important force levels to the tank

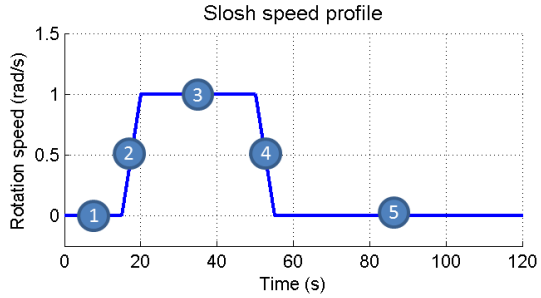

Figure 4 Slosh speed profile shape

CFD validation needs experimental data with high quality and accuracy. It will be provided by an optical system based on high resolution cameras whose fluxes will be recorded in real time and by an effort sensor sensitive to very low loads with a low noise level.

The number of profile is adjusted considering the maximum duration of the sequence limited to 1h30 due to noise regulation in the ISS. The sequence execution has been entirely automatized.

Finally the FLUIDICS experimental setup has also been designed to fulfil the TOC experimental need that consists in recording the fluid height from the tank wall, while the tank is shaken at a frequency around 2 Hz. Tank excitation needs to be as isotropic as possible so that centrifugal acceleration shall be as small as possible compared to tangential acceleration. This leads consequently to a very low amplitude motion.

As a wrap up, FLUIDICS experimental setup is designed to fulfil the functional needs listed in Table 1.

Table 1: functional needs description for FLUIDICS experimental setup definition

Function	Need description
Excite the fluid motion	Generate targeted speed and acceleration profiles
Excite turbulence wave	Generate oscillation with targeted amplitude and frequency
Observe the fluid	Record video fluxes during experimental run
Measure the fluid motion	Record the efforts transmitted from the fluid on the tank and the height of fluid from the tank wall in real time for TOC
Ease manipulation	Minimize the setting and the supervision time

4.2 FLUIDICS overall design presentation

This chapter presents the FLUIDICS hardware designed to fulfil the expressed need in **Erreur ! Source du renvoi introuvable.** while being compliant to all ISS safety rules and to Columbus interface requirements. The design is as much as possible based on commercial products to reduce cost, manufacturing and integration time, and globally follows a prototype approach.
Firstly FLUIDICS includes three different spherical tanks with a diameter of 10 centimetres that can be easily plugged on the FLUIDICS rotating arm and exchanged once the associated test sequence is over.

One of the tanks is dedicated to the TOC experiment, filled with 30% of water and equipped with 2 specific height sensors to instantaneously measure the fluid height. The sensors consist in two taut isolated electrical wires (0.32 mm of diameter). The capacity of each wire is proportional to the wetted length, the water being an electrical ground [6]. Embarked electronic cards measure instantaneously these capacities and deliver analogic signals. After calibration, the fluctuations of the water level are measured with accuracy better than 10 µm. The TOC tank is illustrated on **Figure 5** (left side). The two other tanks are respectively filled with 50% and 75% of 3M Novec 2704 fluid which is an electronic card coating with a yellow aspect as shown on **Figure 5**. This fluid has been chosen in compliance with ISS safety guidelines to provide a representative contact angle compare to satellite propellant to validate the major assumption of no solid-gas interface exists in satellite tank made in the CFD code to simplify equations solving. Viscosity was checked to be not too important so that damping would be long enough to avoid a fast sloshing attenuation. Fluid density was compatible of maximum angular speed available to reach the Bond number range. Tanks are made of 2 polycarbonate half spheres glued together.
Tanks are plugged on the rotating arm through an interface plate linked to a 6 axis force sensor that will give an estimation of the loads and momentum transmitted by the fluid slosh to the tank on all three axes. This sensor is optimized to measure force levels of 1 mN, the expected order of magnitude of sloshing effort. Because of the great sensitivity of the sensor a guiding rail visible on **Figure 6** (right side) and **Figure 7** helps the astronaut to insert the tanks without stress that may cause irreversible damage.

The lever arm between the rotation axis and the tank centre of mass has been set to 180 mm so that the maximum required acceleration is obtained with a safe and quite low rotation speed while complying with the dimension constraint.

Figure 5: TOC tank (left side) and 50% Slosh tank (right side)

On one side, the rotating arm supports the tank under test and the instrumentation to observe and record the fluid motion. This instrumentation consists in two high resolution monochromatic cameras. High resolution cameras lenses with a fixed focal length of 16 mm have been selected to get the full tank diameter covered on the video. When looking at a fixed image, the resolution is 1 mm.
The other side of the rotating arm supports all the electronics needed to record the video fluxes and the sensors data. The core is an Intel NUC computer embedding the FLUIDICS acquisition software that captures the video flux through a high speed USB 3.0 link directly from the cameras.
Height sensor of TOC tank and the force transducer output analogic signals are digitized by a 16 bit high speed DAQ card also connected to the NUC by a USB link.
Signals and video are recorded on the SSD disk.

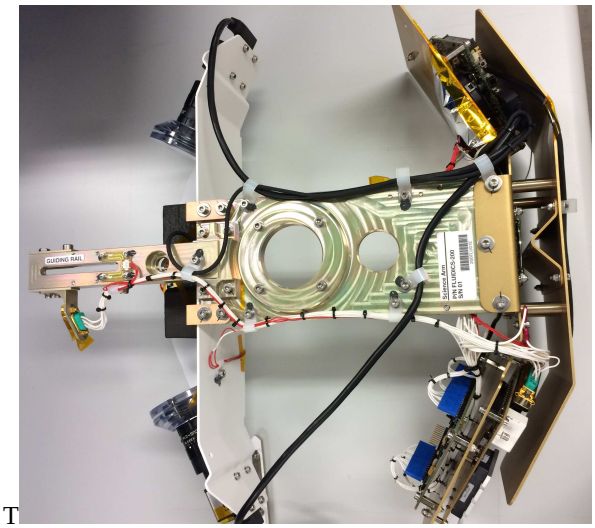

T

Figure 6: FLUIDICS rotating arm

The rotating arm is fixed to the motor block designed to deliver the expected acceleration, speed and position motion of the tank for both slosh and TOC profiles. The motor is a Kollmorgen COTS controlled by its driving electronics from Copley Controls. It can provide a torque up to 1 Nm that corresponds to a maximum angular acceleration of the arm of 10 rad/s^2. The only safety critical function of FLUIDICS is a two failure tolerant speed protection system guaranteeing the motor would not generate a kinetic energy greater than 2 joules. The maximum rotation speed in nominal configuration is 20 rpm. The speed protection system consists in three fully independent monitoring channels

with three inductive sensors to estimate the rotation speed and cut-off the power in case of overspeed detection.

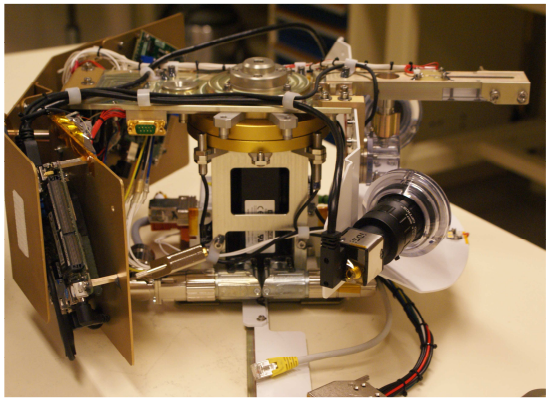

Figure 7: Motor sub-block assembled with the rotating arm

The FLUIDICS setup has also to be robust to potential crew induced loads during operations when not under crew supervision. Potential impacts are modelled by a punctual force of 556N over a 0.5 inch diameter circular area. In order to comply with this rule, the best solution was to protect all the sensitive parts with a box as shown on **Figure 8**. Three buttons have then been installed to control the entire FLUIDICS operations: power on, Intel NUC on/off switch and record start/stop. The Power Supply and Protection Unit (PSPU) in yellow on **Figure 8** are cooled using fans.

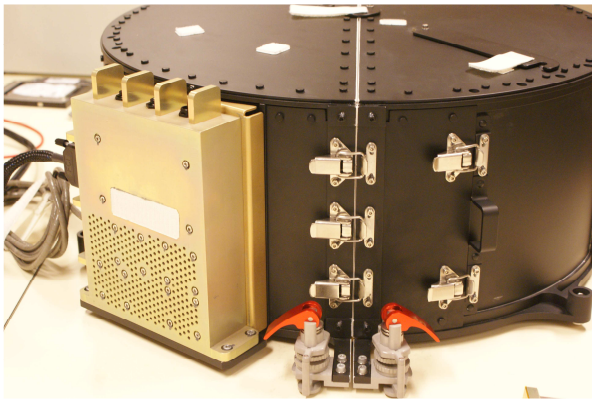

Figure 8 : FLUIDICS protection box

For the operations, FLUIDICS is clamped to the ISS seat tracks using four fixations system designed by Allsafe (initially used for A400M cargo fastening). This system is specially designed to cope with potential misalignment or gaps of the ISS seat tracks. Each of the 3 axis have sufficient margin to ensure a correct and easy clamping of FLUIDICS.

The control of the rotating arm via the motor driver is done according to a guidance profile and performed using a T61P laptop already aboard ISS. From this laptop, software designed for FLUIDICS allows the crew to control the motor and run pre-defined test scenarios.
A Graphical User Interface (GUI) as depicted on **Figure 9** has been developed to ease astronaut's use and monitoring. The GUI plots in real time the position speed and torque based on the data provided by the motor controller.

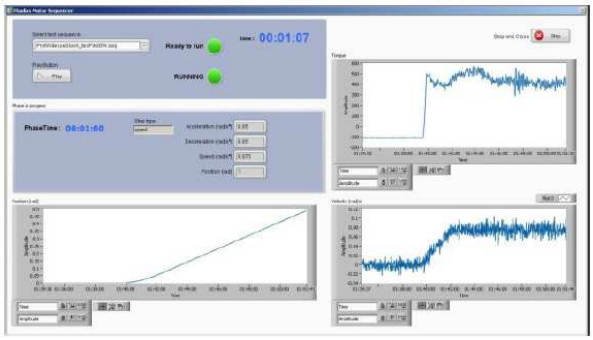

Figure 9 : FLUIDICS motor sequencer software

The crew time dedicated to FLUIDICS experiment shall be limited. Thus, the motor sequencer software and the acquisition software were designed to be fully autonomous: once launched by the astronaut, the sequence is automatically driven and stops at the end. This allows executing 90-minutes tests sequences using a limited crew time.
Volume of recorded data is quite important especially because of two high resolution cameras video fluxes output in the AVI format with 25 frames per second, ground tests give 0.8 Go per minute for the video. Downloading through ISS telemetry should therefore not be possible for video and the nominal solution to get the experimental data is the physical re-entry of data SSD while a backup will remain on-board ISS in case of trouble in the recovery of the first one. The volume of sensor data is far less important and has been estimated on ground to 60 Mo for 10 minutes with a good representativeness so that all or part of text data will be downloaded via standard ISS telemetry.

5. Results

Thomas PESQUET operated FLUIDICS the 2nd and 3rd of May 2017 as shown on Figure 10**Erreur ! Source du renvoi introuvable.**. The setup assembly went as planned without any difficulty encountered. Thomas PESQUET even liked FLUIDICS and made two extra runs. Text files containing the sensor data have been

downloaded via ISS telemetry and a first level of analysis demonstrate the good behaviour of FLUIDICS and the compliance of the provide data.

After the recovery of the SSD disk with Thomas PESQUET return on earth on the 2nd of June 2017 the data analysis started.

Figure 10: Thomas PESQUET operating FLUIDICS

5.1 Slosh result

After having post-processed the FLUIDICS data, the most exploitable profiles were selected to be correlated with CFD simulations. The aim was to set up numerical simulations with the same features as the real FLUIDICS experiment in order to observe how the CFD code deals with sloshing phenomena in microgravity.

A first set of simulations of one profile was carried out using FLOW-3D CFD software. Even though there is some noise remaining on the sensor data, this first comparison with FLOW-3D gives encouraging results. The force in the z-direction is plotted on **Figure 11**. The step is due to the centrifugal force acting on the fluid.

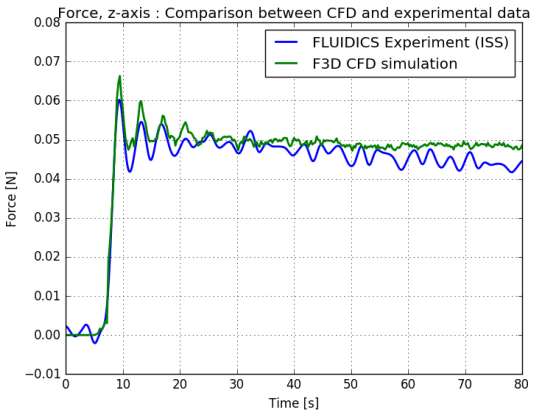

Figure 11: FLUIDICS results and CFD simulation - Force comparison

The sloshing phenomenon is best highlighted by the torque in the y-direction on **Figure 12**. Clear oscillations of the fluid can be seen, whose frequency corresponds to 0.26 Hz. This frequency can also be noticed on the videos from FLUIDICS, so this tends to strengthen the result.

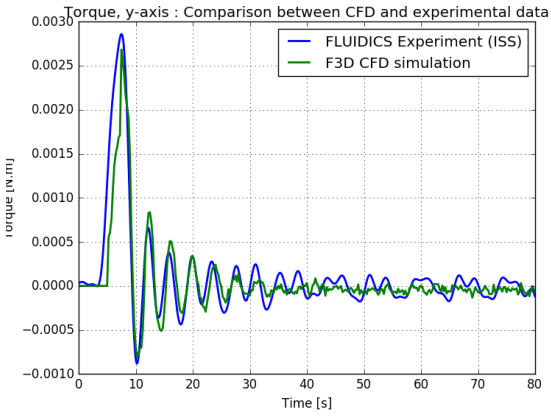

Figure 12: FLUIDICS results and CFD simulation - Torque comparison

This first comparison constitutes the beginning of this analysis. Further simulations now need to be carried out in order to study in detail the influence of the solver options and to make sure that the CFD software computes well sloshing phenomena in microgravity.

5.2 Wave turbulence results

In the experiments performed with the sphere TOC, before excitation, the water wets the internal spherical wall of the sphere in polycarbonate. Without excitation the water is expected to form a spherical shell of 10 cm of external diameter and a thickness of 5.6 mm given the filling ratio of 30%. An oscillatory motion of the tank excites inertially capillary waves. The corresponding fluctuations of the air-water interfaces

are recorded by the two capacitive sensors. The sensor 2 measures the water level at a position opposite to the axis of rotation. The sensor 1 belongs to a plan, which is perpendicular to the axis of rotation and is separated from sensor 2, by an angle of 120°.

Nine different forcing of 450 s each have been tested in a sequence of 5400s. The sequence has been repeated identically two times. To minimize centrifugal effects, which would induce an effective weight, the amplitude of angular displacement θ_0 has been chosen small 2.29° and is kept constant for all runs. The forcing is caused by the tangential acceleration which depends on the oscillation frequency $\mathbf{f_0}$ at the power two, $a_\theta = R\,(2\,\pi\,\mathbf{f_0})^2$, with R=175.4 mm the arm length.

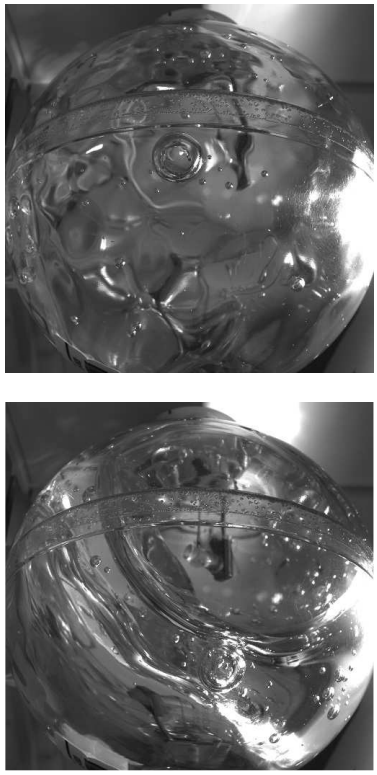

Figure 13: Snapshots of the tank TOC with camera 1, during the second run. Presence of air bubbles is noted. In the bottom image a strong transient dewetting is visible on the top right corner of the spherical tank.

The three first runs correspond to sinusoidal excitations for $\mathbf{f_0}$ being respectively 1.5, 1.75 and 2 Hz. The three following runs are performed with a random modulation of the frequency f on a range about 1 Hz. Finally, in the three last runs, the oscillations have been replaced by sharp impulsions of amplitude $+\theta_0$ and $-\theta_0$ separated by resting times of order 0.4 s (regular or random). The three sinusoidal runs provide a higher motion of fluid surface, probably due to a higher coherence of tank motion and only the corresponding first three measurements are now described.

After starting the forcing sequence, the liquid motion is visualized with the cameras and the local level is measured in two separated points using the two capacitive. Images of the camera 1, shows a strong deformation of the air/water interface in **Figure 13**. However, the significant refraction prevents a quantitative detection of interface position. Moreover, we observe presence of numerous air bubbles trapped in the water. Due to the absence of gravity, bubbles do not migrate spontaneously to the interface. If the motions are sufficiently steep to generate bubbles, their amount would increase in the course of experiments. Then especially on the side of the tank opposed to the axis of rotation, for large scale motions of the fluid, the water layer ceases to wet the internal wall of the tank. These dewetting events last for less than the second.

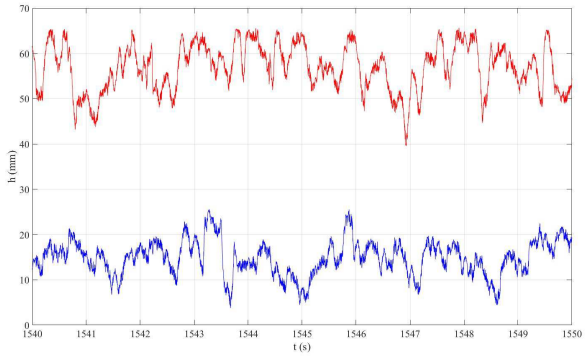

Figure 14 Temporal evolution of water height level for the run 3. Blue sensor 1, Red sensor 2. The signal of sensor 2 has been translated of 35 mm

.

Despite the substantial large scale motion of fluid in the tank, the level fluctuations are well captured by the records of the two capacitive sensors. The repetition of the sequence shows a satisfying reproducibility of measures. The signals are different for the two sensors. The signal of sensor 1, has lower amplitude, seems more affected by the dewetting and presents more features of large scale oscillations. The signal of sensor 2, is sometimes saturated, which means that the sensor is completely immersed in water. The dynamical properties measures are not perturbed by the transient saturation. An example of temporal evolution of water height is displayed in Figure 14 for the run 3 ($\mathbf{f_0}$=2 Hz). A thermal drift of electronic component values may explain, that by using the on Earth calibration, the computed h(t) is not exactly equal to the distance to the

internal tank wall. Dynamics of the interface fluctuations are better described by computing the Fourier power spectrum of h(t). It is defined as the modulus square of the frequency Fourier transform. In the Figure 15 Frequency power spectra of water height fluctuations. Blue : sensor 1, Red : sensor 2. Top run 1, f0=1.5 Hz. Bottom run 3, f0=2 Hz. The black dash line is the power law $f^{-17/6}$. **top**, the spectrum for run 1 ($\mathbf{f_0}$=1.5 Hz) is displayed. The signal is dominated by the peak at 1.5 Hz and harmonics, displaying a global oscillation of the fluid. The high frequency peaks at 25 and 50 Hz are probably not related to the fluid motions, but more likely to mechanical vibrations of the sensors. The signal can be analysed for frequencies below 50 Hz, before reaching noise level. In contrast at higher excitation amplitude for the run 3 (f_0=2 Hz), in Figure 15 **bottom** the peaks from forcing are less strong compared to signal power between them, especially for the sensor 2. The spectrum is then close to becomes continuous and approaches a power-law in $\mathbf{f^{-17/6}}$. A continuous power-law spectrum is a signature of a self-similar turbulent signal, whose traces of forcing do not appear in the inertial range, *i.e.* for frequencies larger than the forcing frequency. The exponent -17/6 ≈ -2.8 is predicted by the Wave Turbulence Theory [3]. This result is in agreement with the previous measurements in parabolic flights [5] and measurements on Earth. But for the last ones, the capillary cascade starts typically for frequencies above 15 Hz and has to be initiated by a random excitation. Here, as the viscous dissipation level is smaller for lower frequencies, the capillary cascade is developed on one decade and half. However, the non-linearity level is significant. It is usually evaluated by computing the typical slope of interface deformation, the steepness, by taking the product of the wave number k_m corresponding to the spectrum maximum multiplied by the standard deviation of wave amplitude. The dispersion relation for pure capillary waves for a sufficiently thick water layer writes $(2\,\pi\,f)^2 = \sigma/\rho\,k^3$, with σ the surface tension coefficient for the interface and ρ the liquid density (the density of air is neglected). We found for f=1 Hz, with σ=72e-3 J/m^2 and ρ=1000 kg/m^3 k_m= 81 1/m and for a standard deviation of signal of 6 mm, the steepness is of order 0.49, which corresponds to a strongly nonlinear regime. The condition of weak non-linearity used in the Weak Turbulence Theory should in principle fails. The high steepness explains also the continuous formation of drops and bubbles by the microbreaking of the interface. Finally, we observe at low frequencies, a strong level in the spectra. Additional non-linear effects may cause emergence of another power law corresponding to a transient energy transfer from injection scale to the large scales and then a statistical equilibrium of large scales [9].

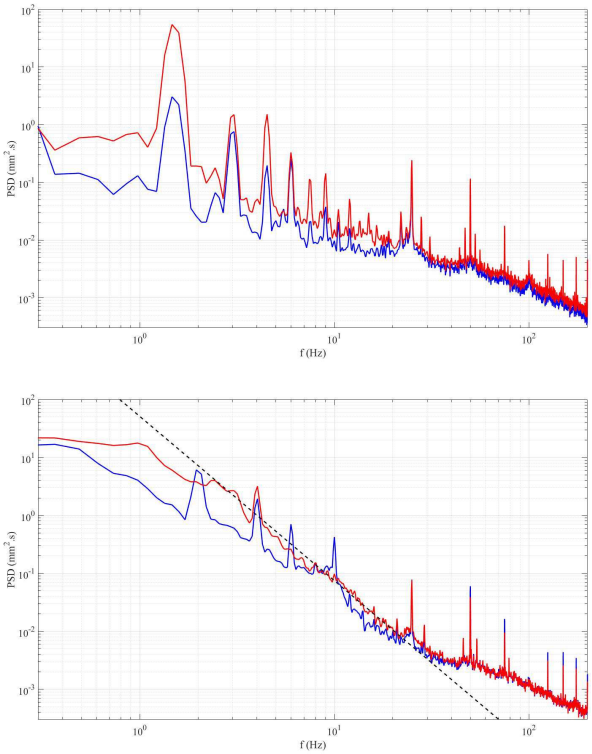

Figure 15 Frequency power spectra of water height fluctuations. Blue : sensor 1, Red : sensor 2. Top run 1, f_0=1.5 Hz. Bottom run 3, f_0=2 Hz. The black dash line is the power law $f^{-17/6}$.

5. Discussion

Next FLUIDICS operations could be handled by the ESA astronaut Paulo NESPOLI to eventually test new profiles.

Experimental data will mainly be used to calibrate and validate CFD code. Videos of the fluid motion inside the tank and forces and momentum transmitted from the fluid on the tank recorded by the 6 axis force sensor are used. For AOCS activities a special focus is put on frequency, damping and magnitude of the efforts generated by the liquid slosh as they directly act as disturbance torque that the AOCS needs to counteract. The CFD Model parameters will be tuned and the physical assumptions made to simplify the equation solving could be reviewed to match as close as possible the experimental results.

Videos will give precious information on various topics that are nowadays not validated. The first point will be the free surface movement correlation when the tank is rotating at a constant angular speed. This will give information on the centre of mass position, the knowledge of which is of prime importance on some

missions to very precisely locate the satellite. The contact angle will also be observed because it is a very important parameter in the CFD code. Indeed it directly determines whether a triple point characteristic of a solid-gas interface can appear. This type of phenomena strongly modifies sloshing characteristics of critical interest for AOCS design and validation such as frequency and damping.

A great variety of profiles could be used to extend the validation domain. Alternative optimized guiding profiles commonly known as “input shaping” of the bang/stop/bang strategy could be investigated and tested in a real environment to reduce as much as possible the slosh impact [7].

New tanks could also be considered to study for instance the efficiency of anti-slosh devices such as membranes. More generally FLUIDICS could be used for any experimental purpose that requires low and controlled acceleration levels compatible with a rotation motion as soon as dimension is less than 10 cm. FLUIDICS offers a good visibility thanks to its optical system providing high resolution films. Force measurements transmitted at the interface with the payload are also available with a very good resolution and accuracy at low level results should be clear and concise.

Capillary Wave Turbulence runs (TOC), have shown at relatively high excitation level, power-law spectra in agreement with the exponent predicted by the Weak Turbulence Theory. However, the corresponding regimes do not satisfy the weak non-linearity assumptions. These results in agreement with laboratory experiments on Earth [10] demonstrate that the power-law spectrum of random capillary waves is surprisingly robust. A more general explanation than the one provided by the Weak Turbulence Theory remains to find. Moreover, experimentally a significant amount of trapped air bubbles and of local dewetting events have been recorded in the videos. These observations could perturb the Wave Turbulence phenomenon and biases in an uncontrolled way the interface position measurement. New runs with lower excitation level and longer initial rest times, would be definitely useful to confirm and extend the present results.

6. Conclusions

In conclusion, an experiment platform designed for acquisition of liquid motion data aboard ISS is in place and ready to be used to improve our knowledge of fluid behaviour in micro gravity. This setup developed in the frame of Proxima mission with the French astronaut Thomas PESQUET should indeed remain on-board and could eventually be operated by other astronauts. This experimental setup will be fully complementary to the Airbus MICROSLOSH hardware that should come soon to focus more specifically on the closed loop aspect.

Meanwhile FLUIDICS more generally provides an easy to use and autonomous experimental setup to investigate the behaviour of any system compatible with the existing interface in a micro gravity environment requiring long duration test.

References

[1] Abramson, H. N., "The Dynamic Behavior of Liquids in Moving Containers", NASA SP-106, 1966

[2] Sunil Chintalapati1, “Design of an Experimental Platform for Acquisition of Liquid Slosh Data aboard the International Space Station”, Florida Institute of Technology, Melbourne, 48th AIAA/ASME/SAE/ASEE Joint Propulsion Conference & Exhibit, 2012

[3] Alan C. Newell and Benno Rumpf “Wave Turbulence”, Annual Review of Fluids Mechanics, **43** (59) 2011
Sergey Nazarenko and Sergei Lukaschuk, “Wave Turbulence on Water Surface” Annual Review of Condensed Matter Physics, **7** (61) 2016

[4] Luc Deike, Daniel Fuster, Michael Berhanu, and Eric Falcon, “Direct Numerical Simulations of Capillary Wave Turbulence”, Physical Review Letters, **112**, 234501, 2014
Yulin Pan and Dick K. P. Yue “Direct Numerical Investigation of Turbulence of Capillary Waves”, Physical Review Letters, **113**, 094501, 2014

[5] C. Falcòn, E. Falcon, U. Bortolozzo and S. Fauve “Capillary wave turbulence on a spherical fluid surface in low gravity”, Europhysics Letters, **86** (1402) 2009

[6] L.F. McGoldrick, “A Sensitive Linear Capacitance to Voltage Converter, with Applications to Surface Wave Measurements”, Review of Scientific Instruments, **42**, 359 (1971);

[7] F. Cirrillo, “Coupled AOCS and CFD analyses for high accuracy fuel sloshing predictions: improvement and validation via ISS experiment”, ESA GNC 10th conference, 2017

[8] Romain Pierre, Rémi Roumiguié, Dorian Lasnet, Jean Mignot, “Fluid dynamics in space experiment ”, ESA GNC 10th conference, 2017

[9].Guillaume Michel, François. Pétrélis and Stéphan Fauve, Physical Review Letters,**118**, 144502 (2017)

[10] Michael Berhanu, Eric Falcon, “Space-Time-Resolved Capillary Wave Turbulence”, Physical Review E, **89**, 033003 (2013)